iScience

CellPress
OPEN ACCESS

Article

# Peptidomic analysis of endogenous and bacterial protease activity in human plasma and wound fluids

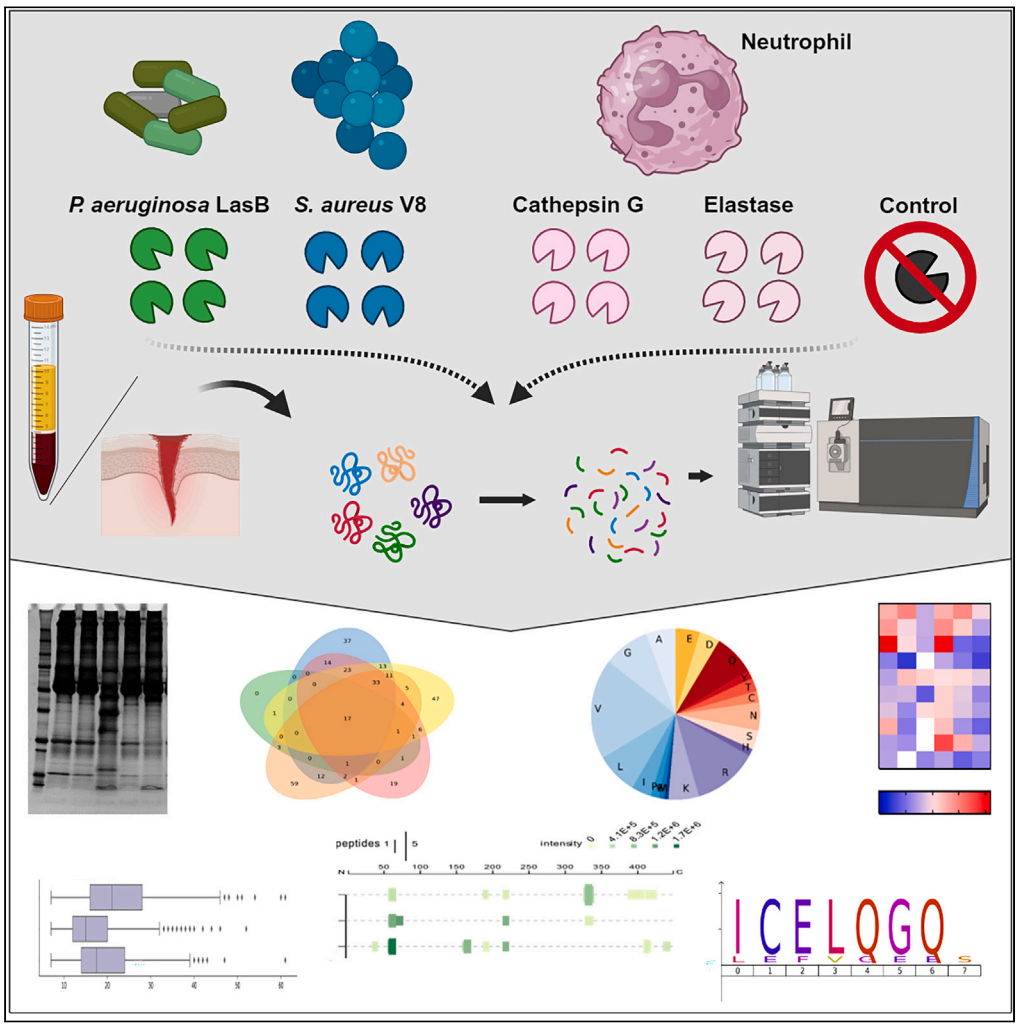


Jun Cai, Maike W. Nielsen, Konstantinos Kalogeropoulos, Ulrich auf dem Keller, Mariena J.A. van der Plas

mariena.van_der_plas@sund.ku.dk

## Highlights

Over 100 protein targets for each enzyme

LasB and V8 cleave antimicrobial peptides with probable consequence for activity

Discovery of potential diagnostic biomarkers for wound infection

Unique peptide regions in V8 samples also detected in *S. aureus* infected wounds

Cai et al., iScience *27*, 109005
February 16, 2024 © 2024 The Author(s).
https://doi.org/10.1016/j.isci.2024.109005

iScience

CellPress
OPEN ACCESS

Article

# Peptidomic analysis of endogenous and bacterial protease activity in human plasma and wound fluids

Jun Cai,[1] Maike W. Nielsen,[2] Konstantinos Kalogeropoulos,[2] Ulrich auf dem Keller,[2,3] and Mariena J.A. van der Plas[1,4,*]

## SUMMARY

**Endogenous and bacterial proteases play important roles in wound healing and infection. Analysis of alterations in the low-molecular-weight peptidome by individual enzymes could therefore provide insight into proteolytic events occurring in wounds and may aid in the discovery of biomarkers. Using liquid chromatography with tandem mass spectrometry, we characterized the peptidome of plasma and acute wound fluids digested *ex vivo* with human (neutrophil elastase and cathepsin G) and bacterial proteases (*Pseudomonas aeruginosa* LasB and *Staphyloccocus aureus* V8). We identified over 100 protein targets for each enzyme and characterized enzyme specific peptides and cleavage patterns. Moreover, we found unique peptide regions in V8 digested samples that were also present in dressing extracts from *S. aureus* infected wounds. Finally, the work indicates that peptidomic analysis of qualitative differences of proteolytic activity of individual enzymes may aid in the discovery of potential diagnostic biomarkers for wound healing status.**

## INTRODUCTION

Skin repair is a highly dynamic but fragile process that involves a series of overlapping and tightly regulated phases. A major complication of healing is bacterial infection, which may lead to prolonged and unregulated inflammation, aberrant protease activity, and subsequent delayed wound closure.[1,2] Furthermore, wound infection poses a risk for unaesthetic scarring, the development of non-healing wounds, and even invasive infections and sepsis, together resulting in a significant economic burden for society as such.[3–5] Balanced endogenous protease activities are of great importance for the progression of wound healing through its phases, whereas aberrant activity caused by both endogenous and bacterial protease may result in delayed healing,[6] as reported for infected acute wounds[7] and non-healing ulcers.[8,9] Indeed, endogenous proteases such as the neutrophil-derived serine proteases human neutrophil elastase (HNE) and cathepsin G (CG) play pivotal roles in the inflammation and proliferation phases of healing, but have been reported as early-stage warning markers for infection and non-healing ulcers too.[10] In clinics, HNE activity in wounds is used as a biomarker to detect wound status and predict healing progression.[11,12]

Dysfunctional endogenous protease activities can be a consequence but also a cause of infection, as it may delay wound closure thereby providing easy entrance for bacteria. Although many bacterial species have been identified in infected wounds, *Staphylococcus aureus* is a commonly found Gram-positive species in both acute and chronic wounds, whereas *Pseudomonas aeruginosa* is one of the most common Gram-negative species in non-healing venous leg ulcers.[13–15] The presence of bacteria impairs wound repair by the release of among others virulence factors such as bacterial proteases that degrade host proteins, thereby damaging the fragile regenerating wound bed. For instance, the metalloprotease *P. aeruginosa* elastase B (LasB) and the *S. aureus* serine protease V8 (SspA) both cleave extracellular matrix components such as fibronectin,[16] vitronectin,[16,17] and laminin α3 LG4-5,[18] as well as inhibitors of endogenous proteases,[17,19,20] thereby enhancing proteolytic activity even further. Moreover, bacterial proteases may influence endogenous proteases directly and work in synergy to amplify the hostile wound environment.[21–24]

As the level of protein degradation is a direct indicator of proteolytic activity, analysis of the resulting peptides may be useful to measure and predict wound healing status. Therefore, we previously developed a mass spectrometry-based method to investigate the low-molecular-weight peptidome of wound fluids.[25] Comparing wound material from non-inflamed, non-infected healing wounds with inflamed and *S. aureus* infected wounds, we showed in a proof-of-concept study that this method can detect subtle qualitative differences in peptide patterns derived from individual patient samples. Furthermore, quantitative analysis of these samples using sorting algorithms and open source software further revealed differences between the non-infected and infected patient samples, while *in silico* prediction of endogenous protease activity showed that both HNE and CG were important contributors of the observed cleavages in the infected wound samples.[26] As different proteases have different

[1]LEO Foundation Center for Cutaneous Drug Delivery, Department of Pharmacy, University of Copenhagen, 2100 Copenhagen Ø, Denmark
[2]Department of Biotechnology and Biomedicine, Technical University of Denmark, 2800 Kgs. Lyngby, Denmark
[3]Deceased in August 2023
[4]Lead contact
*Correspondence: mariena.van_der_plas@sund.ku.dk
https://doi.org/10.1016/j.isci.2024.109005


This is an open access article under the CC BY-NC-ND license (http://creativecommons.org/licenses/by-nc-nd/4.0/).

substrate specificities, and therefore will degrade endogenous proteins into peptides with enzyme specific cleavage site characteristics, the observed differences between the patient groups are likely explained by the level and nature of both endogenous and bacterial proteases in these wounds. Thus, characterization of the individual contributions of proteases may reveal unique peptides and patterns that, when present in patient samples, could provide hints on the harmful presence of endogenous and/or bacterial protease activities, and may be used as potential diagnostic and prognostic biomarker candidates to measure wound status and predict healing. Therefore, the aim of this study was to investigate endogenous and bacterial protease targets in plasma and wound fluids, to identify unique enzyme specific peptides and peptide patterns, and finally to determine the usefulness of such studies for the identification of peptide-based biomarker candidates. For this purpose, we incubated plasma and sterile acute wound fluids *ex vivo* with different concentrations of the endogenous proteases HNE and CG, or the bacterial proteases *S. aureus* V8 and *P. aeruginosa* LasB, and compared their activities by analyzing the resulting peptidomes (or degradomes). We first standardized the enzyme/substrate ratio and optimized our sample preparation for the plasma samples. Then we compared the samples of three different donors and identified individual enzyme targets and unique peptides and patterns in both plasma and wound fluids. Finally, we identified unique peptide regions in V8 digested samples that were also present in *S. aureus* infected wound fluids.

## RESULTS

### Determination of proteinase – sample ratios for digestion

To investigate the individual contributions of selected proteases to the low-molecular-weight peptidome generated in early wound healing processes and acute infection, we mimicked the physiological proteolytic activities in acute (infected) wounds by incubating citrated plasma with endogenous or bacterial proteases. For this purpose, we selected the two endogenous serine proteinases HNE and cathepsin G (CG), secreted from neutrophils in the early stages of healing, and two bacterial proteases, i.e., the serine protease V8 from *S. aureus*, and the metalloprotease elastase (LasB) from *P. aeruginosa*, two bacteria commonly found in infected wounds. In an effort to standardize protease activity, plasma was incubated with a range of each enzyme for 24 h at 37°C, followed by visualization on SDS-PAGE. Next, we selected the lowest concentration of each enzyme that resulted in visible alterations of the band patterns, as compared to the undigested 24 h incubated control, which was then designated as 'low' protease activity. For the endogenous proteases, these concentrations were 3.33 μg of HNE and 5.55 milliunits of CG per 1.00 mg of plasma, whereas for the bacterial proteases, we used 33.33 milliunits of LasB and 0.17 units of V8 per 1.00 mg of plasma. As proteolytic activity may be high in wounds, we also selected a 'high' condition, which was 10x higher amounts of each protease. Notably, distinct differences in cleavage patterns can be observed for the different enzymes (Figures 1A and S1).

### Sample preparation optimization

In classical proteomics, proteins are trypsinized before analysis and hence mainly report on the presence of proteins as such, whereas information about endogenous proteolytic activity and the resulting peptides is lost. In wounds however, endogenous protein degradation is of high relevance for the understanding of healing and therefore we previously developed a method to analyze the low-molecular-weight peptidome of wound fluids.[25] For plasma, we only found very low numbers of proteins and peptides, and therefore we first investigated whether we could optimize our method for these samples. For this purpose, we changed the urea buffer containing *Rapi*Gest SF, a surfactant that increases the solubility of hydrophobic peptides, to a guanidinium chloride (GdCl) buffer containing tris (2-carboxyethyl) phosphine (TCEP) and 2-chloroacetamide (CAA), which reduces and alkylates cysteines, and therefore prevent the reformation of disulfide bonds which may interfere in ms identification. This approach resulted in a 4- to 10-fold increase in the number of identified peptides in plasma samples and a 2- to 5-fold increase in the number of proteins (Figure 1B). As there was no clear difference between using 50 μL and 100 μL plasma as starting material, we decided to continue with 50 μL of sample, which corresponded to 2.7 mg of protein. Next, we tested if the GdCl buffer would also increase the number of identified peptides in wound fluids, but instead we found an 8% decrease (from 539 to 496 peptides) when starting with 50 μL of wound fluid. Therefore, we decided to continue using the Urea+*Rapi*Gest buffer for the wound fluid samples. The other steps in the workflow were similar for the two buffers as indicated in Figure 1C.

### Comparison of protease activities in plasma samples

To compare the individual contributions of the different proteases to protein fragmentation, plasma samples (2.7 mg of protein each) from three donors were incubated for 24 h at 37°C with low and high ratios of each enzyme, or no enzyme as a control, followed by the workflow above and individual database searches for each sample.

Pooling the results into the five groups (undigested 24 h control, HNE, CG, LasB and V8), combining both low and high ratios for all three donors, we found clear differences in identified proteins and peptides as expected (Figure 2A). Indeed, 3- to 4-fold higher numbers of proteins and 4- to 9-fold higher numbers of peptides were detected after HNE (3600 peptides, 149 proteins), CG (4370 peptides, 123 proteins), LasB (6185 peptides, 163 proteins) or V8 (7155 peptides, 162 proteins) treatment as compared to the undigested control samples (753 peptides, 25 proteins). Moreover, only very few peptides and proteins were identified in all groups, suggesting significant alterations in the low-molecular-weight plasma peptidome after protease digestion. In agreement, analysis of the start AA (N-terminal; P1′ position) and end AA (C-terminal; P1 position) amino acids of the identified peptides per enzyme (Figure 2B), as well as the cleavage environment of each cleavage condition separately using iceLogo[27] (Figure 2C), showed substrate specificity of the proteases. Indeed, V8 is known to cleave peptide bonds exclusively on the carbonyl side of the negatively charged (in yellow) glutamate (E) and exhibits some activity for aspartate (D) residues.[28] For CG, we found that the percentages of the positively charged (in purple) lysine (K), the non-polar amino acids (in blue) phenylalanine (F), leucine (L) and methionine (M), and the

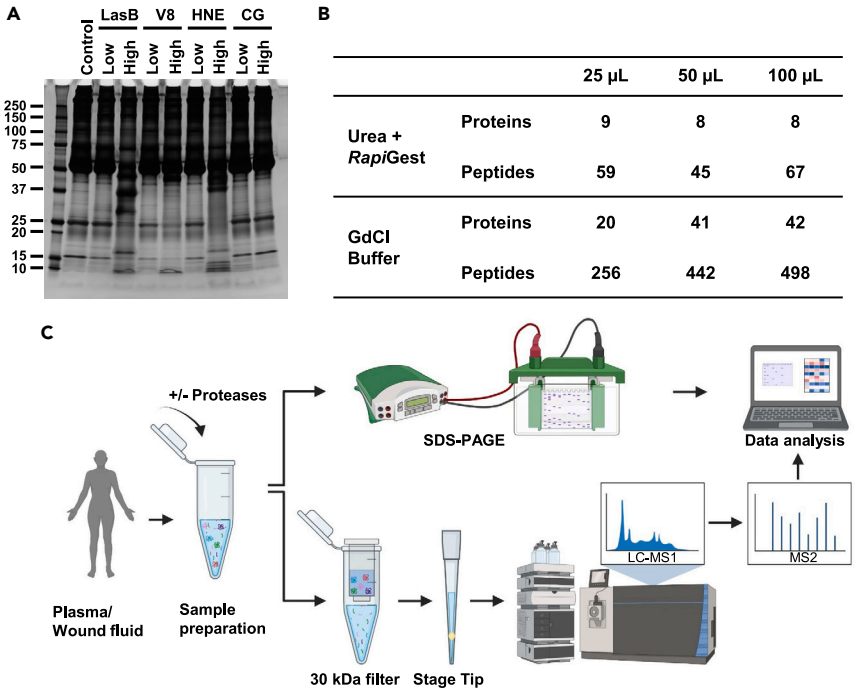


**Figure 1. Preparation of plasma samples**

(A) Plasma was incubated for 24 h at 37°C with a low and high ratio of the proteases LasB, V8, HNE, and CG, and run on SDS-PAGE (see also Figure S1).

(B) Peptides were extracted from 25, 50, and 100 µL plasma in either 6M urea containing 0.05% *Rapi*Gest, or in GdCl buffer containing TCEP and CAA, using 30 kDa cut-off filters. Total numbers of identified proteins and corresponding peptides are shown for the different buffers and amounts of plasma as analyzed by LC-MS/MS.

(C) Schematic overview of the workflow for further studies (created with Biorender.com). Samples were incubated for 24 h, and then either analyzed by SDS-PAGE directly, or filtrated and stored for further processing as above. Stored filtrates were defrosted, followed by peptide concentration/clean-up using StageTips and finally 500 ng of each sample was analyzed by LC-MS/MS.

non-charged polar (in red) tyrosine (Y) significantly increase at the C-terminal position after digestion, as reported.[29,30] In agreement, for HNE there is a significant increase in percentages of the non-polar valine (V), alanine (A), and isoleucine (I), as well as the non-charged polar threonine (T), at this position, as found previously.[30–32] Interestingly, we also found an increase in cysteine (C). Finally, for LasB no clear specificity could be observed at the C-terminal amino acid cleavage side, although glycine (G), proline (P), threonine (T), serine (S), lysine (K) and glutamate (E) were all significantly increased as compared to the control. At the N-terminal position, a substantial increase in non-polar amino acids leucine (L), valine (V), isoleucine (I), phenylalanine (F) and tryptophan (W), as well as the non-charged polar tyrosine (Y) was observed for LasB as reported.[33] Less pronounced but significant changes in the cleavage environment can be observed on all eight positions around the cleavage site for all cleavage conditions.

Notably, all identified peptides are listed in Data S1, while a summary of the total numbers of identified unique peptides, proteins, different modifications, and the average mass and number of amino acids (AA) of the identified peptides is provided in Table S1.

Next, we compared all samples individually. Heatmaps were generated, containing the proteins that were found in all three samples of at least one group, which were then ordered on localization or function. The results show clear differences between the different proteases, as well as between the low and high amounts of these enzymes (Figure 3A). Analysis of the peptide length shows that protease digestion decreases the variation in the median length between the three donors as compared to the undigested control samples (Figure 3B). As expected, increasing the amount of V8, CG, and HNE, from low to high, decreased the median lengths of the identified peptides. By contrast, the median length of peptides identified in the presence of high amounts of LasB were slightly higher than in the low LasB samples, suggesting that larger proteins and peptides were cleaved and came within the detection range of the LC-MS/MS.

Notably, as plasma itself may contain active proteases, we also compared fresh non-incubated (0 h) plasma samples with the control (24 h incubated) plasma and indeed found some autodigestion of the plasma samples after 24 h, both visually on SDS-PAGE and after LC-MS/MS data analysis (Figure S2), although no clear patterns were observed between the donors. Moreover, the variation between the three donors was substantial.

## Determination of bacterial proteinase activity in acute wound fluids (AWFs)

To further investigate the low-molecular-weight peptidome generated during wound infection, we incubated 2.7 mg of sterile AWFs from three donors with LasB and V8 for 24 h, followed by sample processing and analysis. As expected, SDS-PAGE analysis showed more abundant

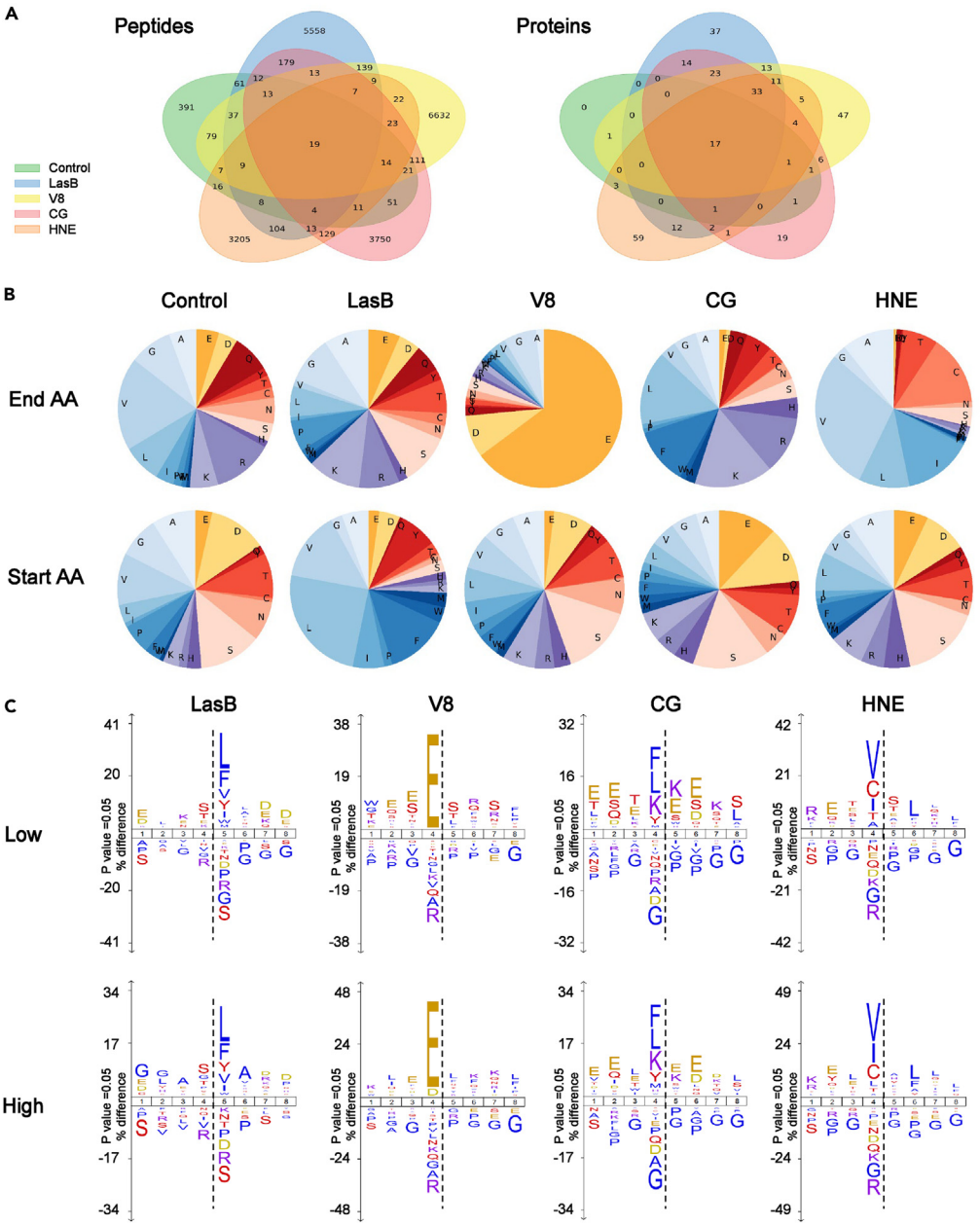


**Figure 2. Comparison of protease activities in plasma samples**

Peptides were extracted from 2.7 mg plasma, incubated for 24 h at 37°C with the indicated enzymes, in GdCl buffer and processed using the workflow in Figure 1.

(A) Comparison of the pooled results of the low and high ratios of each enzyme incubated with plasma preparations of three donors, using Venn diagrams depicting the total number of identified proteins and unique peptides.

(B) Pie charts showing the average distribution of the start (N-terminal) and end (C-terminal) amino acids of the identified peptides in the different samples. The pie charts are categorized into four groups based on the polarity and acidity of the amino acids: negatively charged in yellow, positively charged in purple, non-charged polar in red, and non-polar in blue.

(C) Icelogos depicting the cleavage environment for each condition as compared to the control. The dashed line indicates the cleavage site. See also Figure S2.

low-molecular-weight peptide bands for the samples treated with the proteases, irrespective of the ratio of protease used, as compared to the 24 h incubated control (Figure 4A). Notably, no clear visual differences were observed on SDS-PAGE between the 0 h and 24 h incubated AWF samples for any of the three donors, although LC-MS/MS analysis showed differences in the number of identified proteins and peptides, the median peptide length, and the amino acid distribution (Figure S3) indicating some autodigestion of the samples. Also, a substantial difference was observed between the donors.

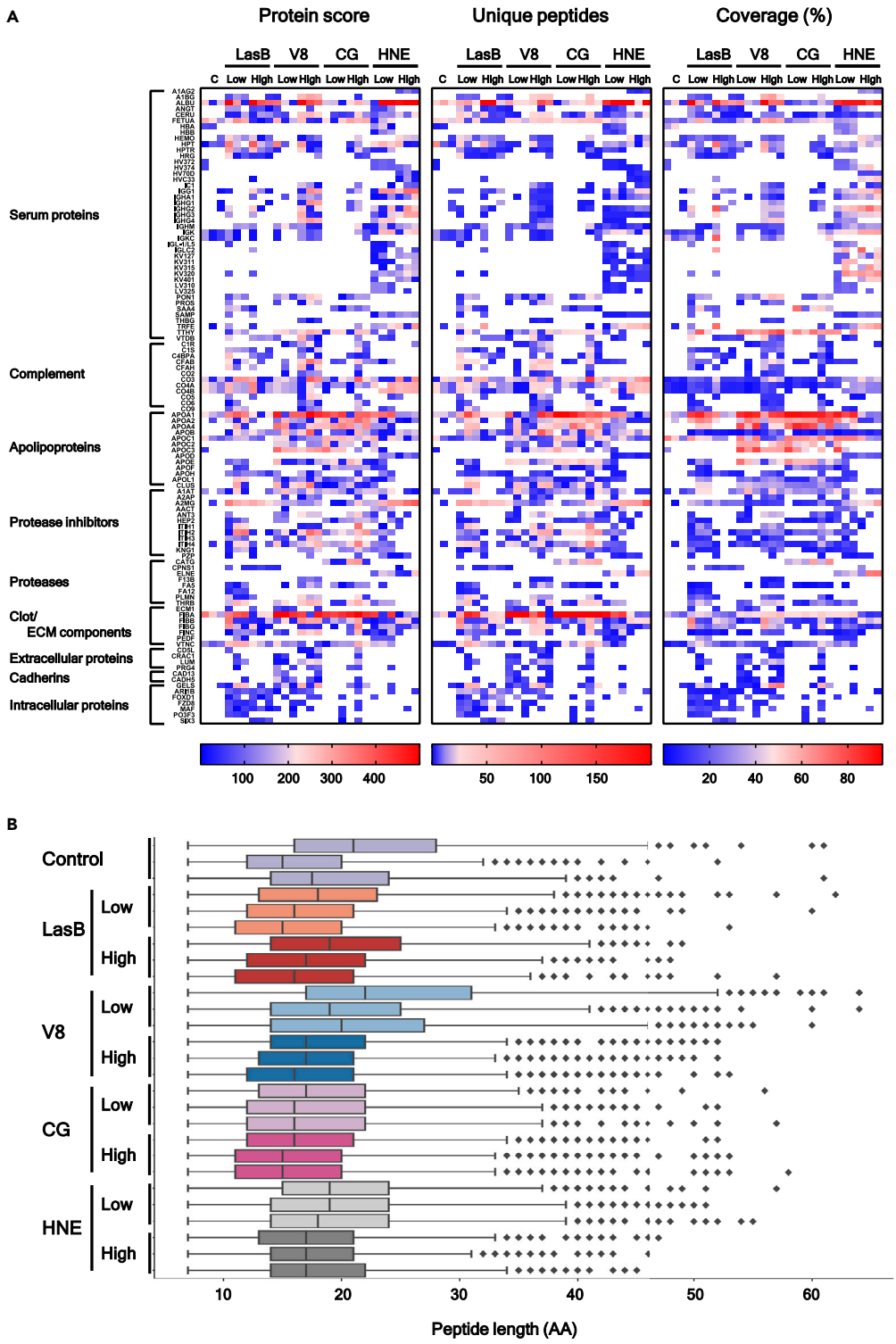


**Figure 3. Comparison of the plasma peptidome of different enzyme ratios**

(A) Heatmaps comparing the enzyme-digested plasma from three donors depicting the protein score, the number of unique peptides per protein and the percentage of total coverage of each protein by the identified peptides. Only proteins are included that were identified in all three donors of at least one of the enzyme groups or control.

(B) Box-plots showing the amino acid length of the peptides identified in each sample. Center lines show the medians; box limits indicate the 25th and 75th percentiles as determined by R software; whiskers extend 1.5 times the interquartile range from the 25th and 75th percentiles, outliers are represented by dots.

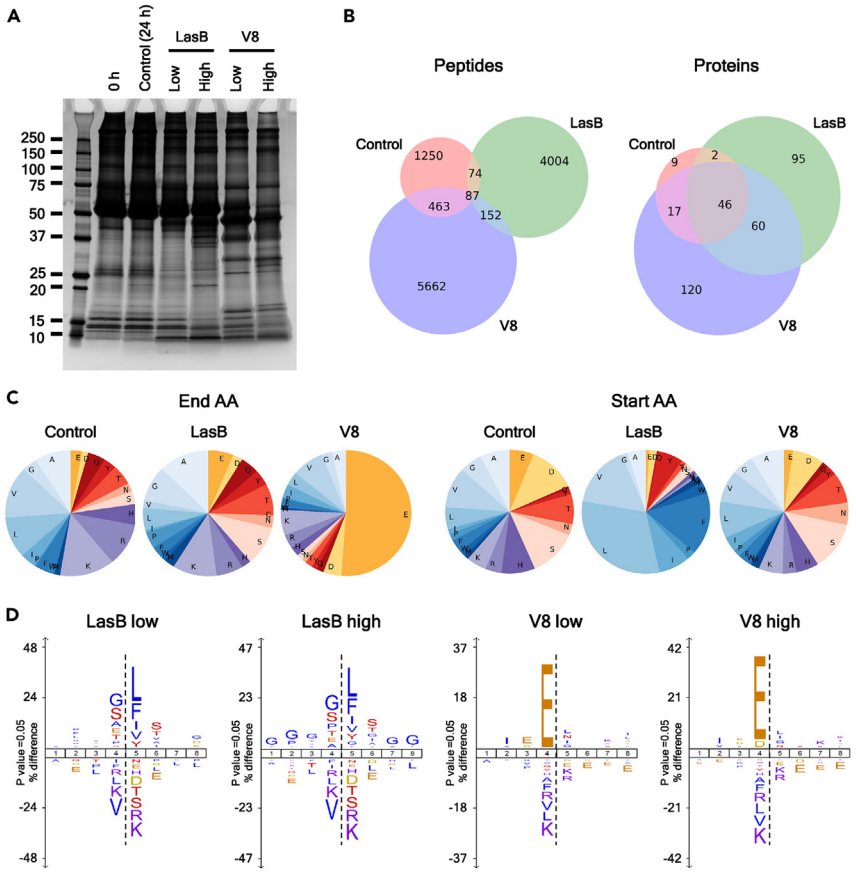


**Figure 4. Comparison of protease activities in acute wound fluids**

Peptides were extracted from 2.7 mg sterile wound fluids, incubated for 24 h at 37°C with the indicated enzymes, in 6M urea supplemented with 0.05% *Rapi*Gest and processed using the workflow above.

(A) Representative SDS-PAGE gel of the digested wound fluids.

(B) Comparison of the pooled results of acute wound fluid preparations of three donors, incubated with the low and high ratios of each enzyme, using Venn diagrams depicting total number of identified proteins and unique peptides.

(C) Pie charts showing the average distribution of the start and end amino acids of the identified peptides in the different enzyme-digested acute wound fluid samples. The pie charts are categorized into four groups based on the polarity and acidity of the amino acids: negative in yellow, positive in purple, non-charged polar in red, and non-polar in blue.

(D) Icelogos depicting the cleavage environment for each condition. The dashed line indicates the cleavage site. See also Figure S3.

Further analysis of the digested AWF samples, by merging the results for all donors and enzyme ratios, showed a 2.7-fold increase in the numbers of proteins and a 2.3-fold increase in peptides after digestion with LasB, whereas for V8 treatment a 3.3-fold increase in proteins and 3.4-fold increase in peptides was observed as compared to the undigested samples (Figure 4B). Interestingly, only 13% (46 out of 349) of all proteins and less than 1% (87 out of 11692) of all peptides were found in all three groups, indicating extensive modifications of the peptidome. Moreover, the results show a significant difference in substrate specificity for LasB and V8, as only 2% (239 out of 10442) of the peptides were found in the samples of both groups. In agreement, analysis of the distribution of C- and N-terminal amino acids for all identified peptides in the three groups (Figure 4C), as well as the cleavage environment of each cleavage condition separately (Figure 4D), showed similarly to the plasma samples, a clear increase in glutamic acid (E), and to a lesser extend in aspartic acid (D), as the C-terminal amino acid after digestion with V8 as compared to the control. For LasB, the results show a similar shift as observed for the plasma samples, with a substantial increase in non-polar amino acids leucine (L), valine (V), isoleucine (I), and phenylalanine (F), as well as the non-charged polar tyrosine (Y), at the N-terminal position.

## Comparison of low and high protease activities on sterile wound fluid samples

To further analyze the contributions of the proteases on the low-molecular-weight peptidome of individual wound fluids, heatmaps were generated (Figure 5A) containing all proteins that were found in all three samples of at least one of the three groups (control, LasB or V8). Interestingly, no obvious shifts in identified proteins, the number of unique peptides from these proteins, or the percentage of protein

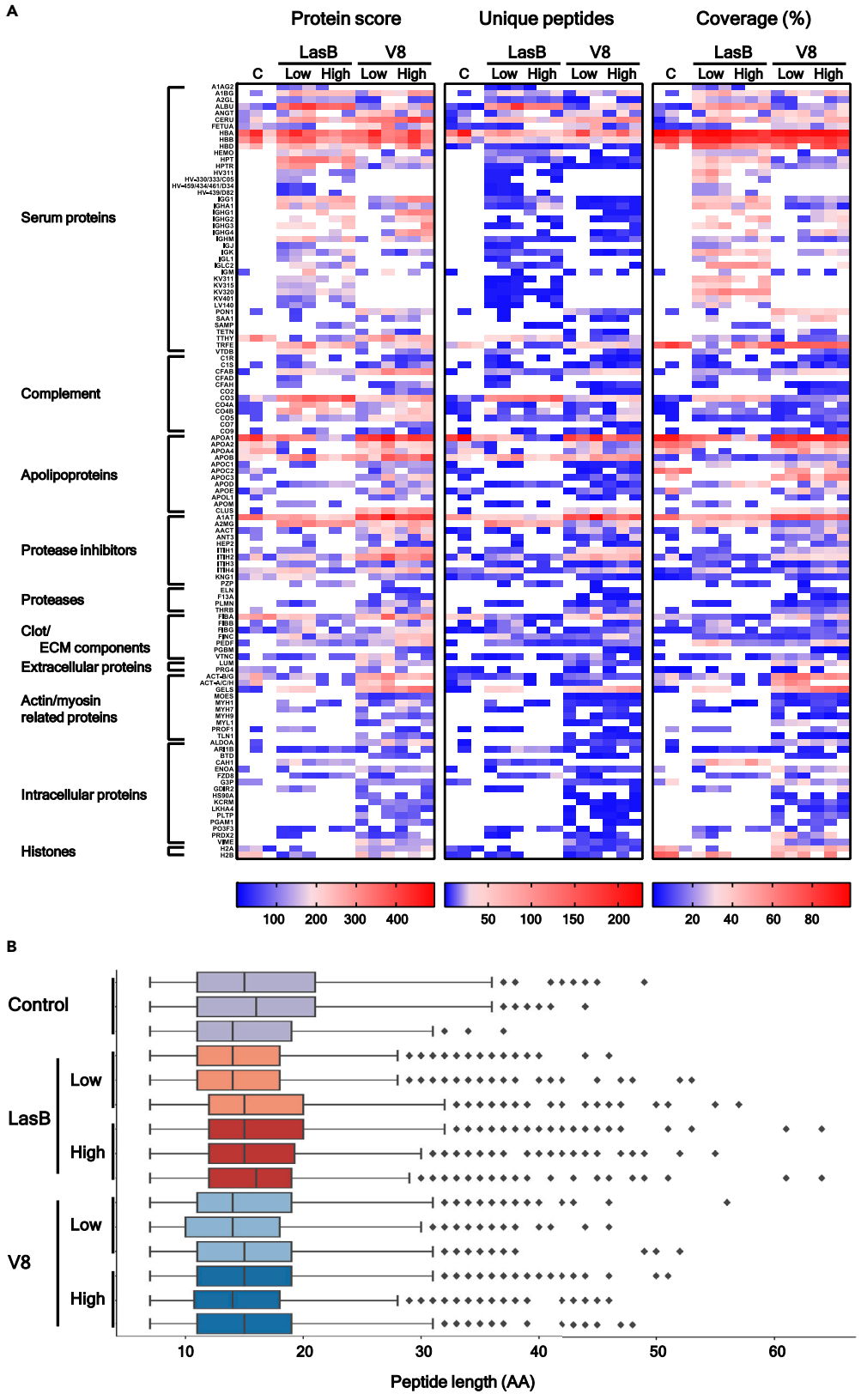
A
Protein score
Unique peptides
Coverage (%)
LasB
V8
C
Low
High
Serum proteins
Complement
Apolipoproteins
Protease inhibitors
Proteases
Clot/
ECM components
Extracellular proteins
Actin/myosin
related proteins
Intracellular proteins
Histones
100 200 300 400
50 100 150 200
20 40 60 80
B
Control
LasB
V8
Low
High
10 20 30 40 50 60
Peptide length (AA)

**Figure 5. Comparison of the wound fluid peptidome of different enzyme ratios**

(A) Heatmaps comparing the enzyme-digested acute wound fluids from three donors, depicting the protein score, the number of unique peptides per protein and the percentage of total coverage of each protein by the identified peptides. Only proteins are included that were identified in all three donors of at least one of the enzyme groups or control.

(B) Box-plots showing the length of the peptides identified in each sample. Center lines show the medians; box limits indicate the 25th and 75th percentiles as determined by R software; whiskers extend 1.5 times the interquartile range from the 25th and 75th percentiles, outliers are represented by dots.

coverage by these peptides were observed when comparing the low and high ratio of each enzyme. However, several proteins, such as serum protein FETUA (fetuin-A), complement component C1s, protease inhibitor KNG1 (kininogen-1), protease PLMN (plasminogen/plasmin), and histone H2B, were identified in the low LasB but not in the high LasB samples, indicating extensive degradation in the latter beyond the lower detection limit of the LC-MS/MS. For V8 on the other hand, the opposite was observed, as various proteins (IGHG1, CO7, FIBB, and PGBM) were only detected in the high enzyme samples.

When comparing the two enzymes, more peptides from serum proteins, especially from the immunoglobulin light chains (IGL, KV-XXX, LV140) and the variable domain of the heavy chains (HV-XXX) were identified after digestion of the wound fluids with LasB, whereas V8 treatment resulted in an increase of peptides derived from apolipoproteins, proteases, and intracellular proteins. Comparison of the median peptide lengths revealed differences between the three donors, which became less pronounced after protease digestion (Figure 5B). Similar to the plasma experiments, the median lengths were slightly higher for the high LasB samples as compared to the low ones. For V8 however, there was no clear difference between the low and high ratios.

Notably, all identified peptides are listed in Data S2, while a summary of the total numbers of identified unique peptides, proteins, different modifications, and the average mass and number of amino acids is provided in Table S2.

## Comparisons of enzyme specific peptide patterns in plasma and wound fluids

To further investigate qualitative differences in protease activity on the peptide level, we selected a number of proteins, based on the heatmap results, and generated peptide profiles of all peptides that were not post-translationally modified (Figures 6, 7, and 8). As expected, clear donor-independent changes in the protein fragmentation patterns occurred, which are the result of substrate specificity of the enzymes, although it can be observed as well that the bacterial enzymes do not cleave proteins to a similar extent in plasma and wound fluids. Notably, many peptides identified after HNE and CG digestion of plasma were not identified in the wound fluid control samples. This discrepancy may be due to low levels of these two neutrophil-derived proteases in the AWFs, whereas higher levels of enzymes were used in our study.

Fibrinogen, a major coagulation factor in plasma, plays important roles during wound healing.[34] It contains two sets of three different peptide chains (alpha, beta, and gamma). As shown in Figure 6, all enzymes can degrade the fibrinogen beta chain (FIBB). Previously, we showed the presence of the antimicrobial and immunomodulatory peptide region GHR28 in healing wounds, whereas truncations were found in infected and inflamed wounds.[25,35] Here we detected mainly these shorter fragments in plasma and wound fluids after digestion with the proteases (blue box), indicating that the biological function of these peptides may be short-lived in a proteolytic environment, which will be beneficial for bacterial infection. Interestingly, peptides starting with N-terminal $^{340}$LLIE were found solely and abundantly in all LasB-digested samples (orange box), which makes this peptide a potential biomarker candidate for *Pseudomonas aeruginosa* infections.

High-molecular-weight kininogen is a 120 kDa glycoprotein which consists of six domains (D1 to D6) that have distinct functions.[36] Domains D2 and D3 inhibit cysteine proteases, while D4 domain contains the sequence of bradykinin, which is released by plasma kallikreins during contact activation and the actions of proteases such as mixtures of HNE and mast cell tryptase.[37] D5 domain is known to contain antimicrobial sequences, of which the peptide LDD40 was reported to be released by LasB.[38] Indeed, truncated versions of this peptide were identified in the 'low' LasB digested plasma and wound fluid samples (blue box), although they were no longer detectable in the 'high' samples (Figure 5A) indicating full degradation. In the control acute wounds, we found similar LDD peptides, which we previously also detected in wound dressings of surgical wounds.[25] As LasB isn't present in these wounds, these observations can be explained by our finding that CG releases these peptides too.

Fetuin-A (FETUA) is categorized as an acute phase protein in response to infection or injury.[39] We previously identified two unique peptides of this protein, one ($^{288}$LPPA) in all three samples of inflamed *S. aureus* infected wound dressing extracts and the other ($^{300}$LLAA) in all three noninflamed and noninfected samples.[25] Interestingly, here we find peptide $^{288}$LPPA and truncated versions of this peptide in the V8-digested AWF samples. In the plasma samples, V8 resulted in the formation of peptides starting with $^{293}$SPPD (orange arrow), which were also found in all V8 wound fluid samples (and in one of the *S. aureus* infected samples), together indicating that this region may contain potential biomarker candidates for *S. aureus* infection. Notably, reduced levels of both fetuin-A and -B have recently been reported as biomarkers for *S. aureus* bacteremia mortality,[40] which may be explained by the proteolytic actions of V8, but also those of the neutrophil-derived proteases. Moreover, it was shown in mice that administration of fetuin-A rescued the animals from cecal ligation and puncture-induced lethal systemic inflammation.[41]

Further evidence of unique proteolytic peptide patterns is provided by proteins of the complement system, a fundamental defense system that is activated during wounding and infection to help remove invading pathogens and damaged host cells. The activation of the complement cascade can be achieved via three different pathways. These are converging at the activation of component 3 (CO3), which results in the release of the anaphylatoxin C3a (residues 672–1663) and the opsonin C3b (residues 23–667), followed by the formation of C5 convertases, which cleaves complement 5 (CO5) to generate the anaphylatoxin C5a (residues 678–1676) and the opsonin C5b (residues 19–673), which is part of the membrane attack complex (MAC; C5b-9).[42] As shown in Figure 7, CO3 and CO5 are both cleaved, although the extent of

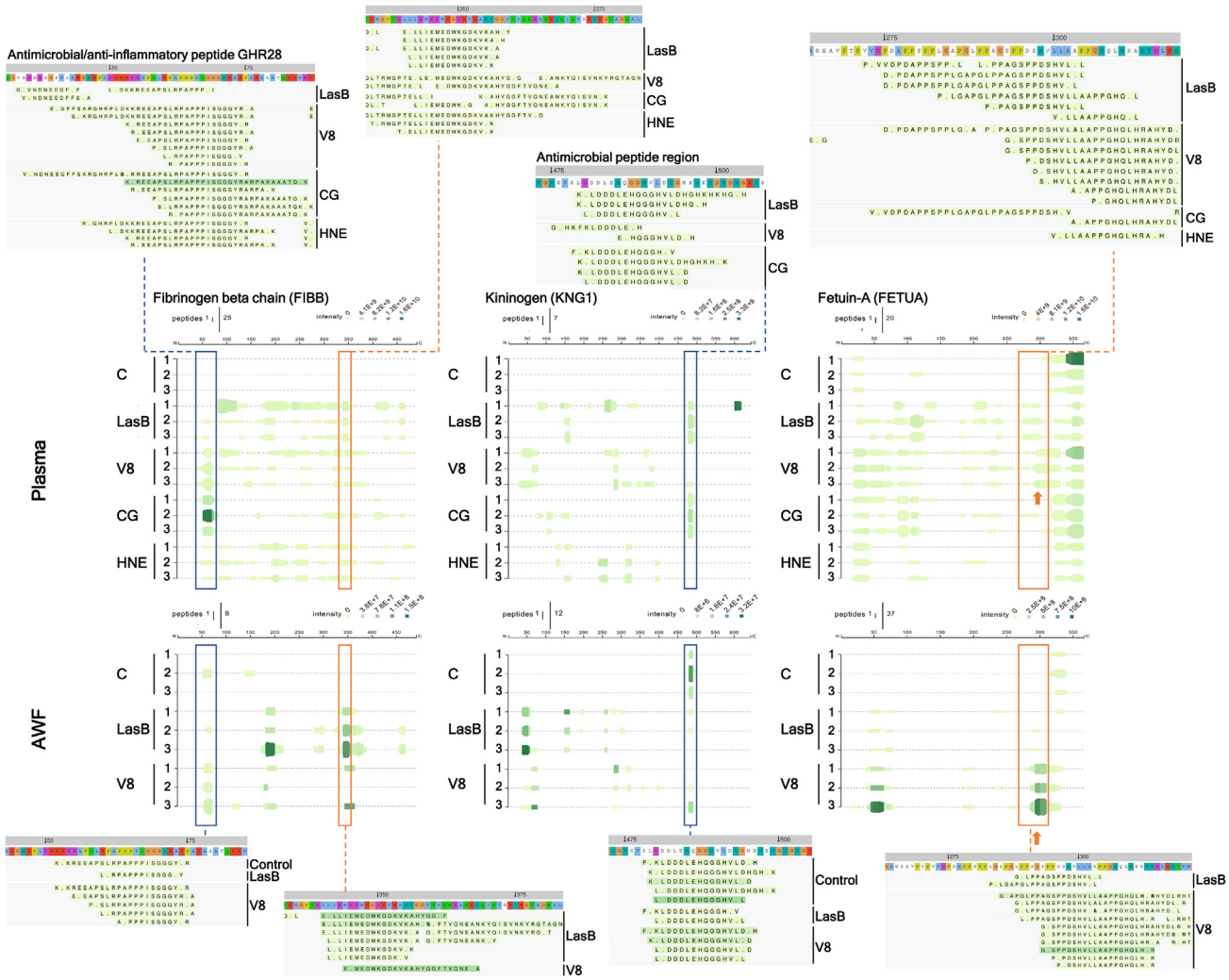


**Figure 6. Peptide profiles for fibrinogen beta chain, kininogen and fetuin-A**

Peptide profiles and peptide alignment maps were generated for the plasma and acute wound fluid (AWF) samples, and interesting peptide regions are highlighted by blue and orange boxes. A selection of the identified peptides is shown for illustration purposes. The arrows indicate peptides unique to the V8-digested samples.

degradation is very different. For CO3 in plasma, both bacterial enzymes and CG predominantly cleaved C3a, whereas HNE showed the greatest fragmentation of C3b. In wound fluids however, LasB cleaved C3b extensively as well. As CO3 is likely activated in the wound fluids, but not in the plasma samples, release of C3b from full length CO3 might be required for efficient LasB proteolysis. For CO5, a very different pattern occurs, as the two endogenous proteases did not release peptides from CO5 in plasma. For V8, a specific cleavage pattern of C5a can be observed in plasma and wound fluids (orange boxes), with peptides starting with $^{943}$TLDP, $^{959}$FPYR, $^{963}$IPLD, $^{996}$GINI, $^{1027}$TGNH and $^{1121}$NSQY found in both types of samples. Notably, cleavage of CO5 by LasB was only evident in wound fluids, and mainly observed for C5b. Interestingly, it has been reported that cleavage of complement components by V8 and LasB aid in bacterial evasion of the immune system.[43,44]

Another group of abundant proteins are apolipoproteins, which are multifunctional proteins that are known for their roles in lipid metabolism and transport.[45] ApoB is the primary protein of the 'bad' cholesterol types VLDL and LDL, but also plays a protective a role in *S. aureus* infections.[46] Interestingly, V8 induced extensive fragmentation of ApoB in both plasma and wound fluids (Figure 8), which would likely abolish its protective role. Furthermore, the other tested enzymes all degraded ApoB as well, with several unique peptides for each enzyme. Analysis of the ApoB peptides identified in the patient samples from our previous study[25] revealed similar peptide fragments in *S. aureus* infected wound fluids and V8 digested AWF, but not digested plasma, with various peptides starting with $^{2622}$TDLR and $^{3724}$KVLA present in both types of samples, making these potential biomarker candidates. Apolipoprotein E (ApoE) is another multifunctional protein which exerts antimicrobial activity.[47] Synthetic ApoE-derived peptides from residues 130–150 have antibacterial and antiviral activity,[48–50] as well as

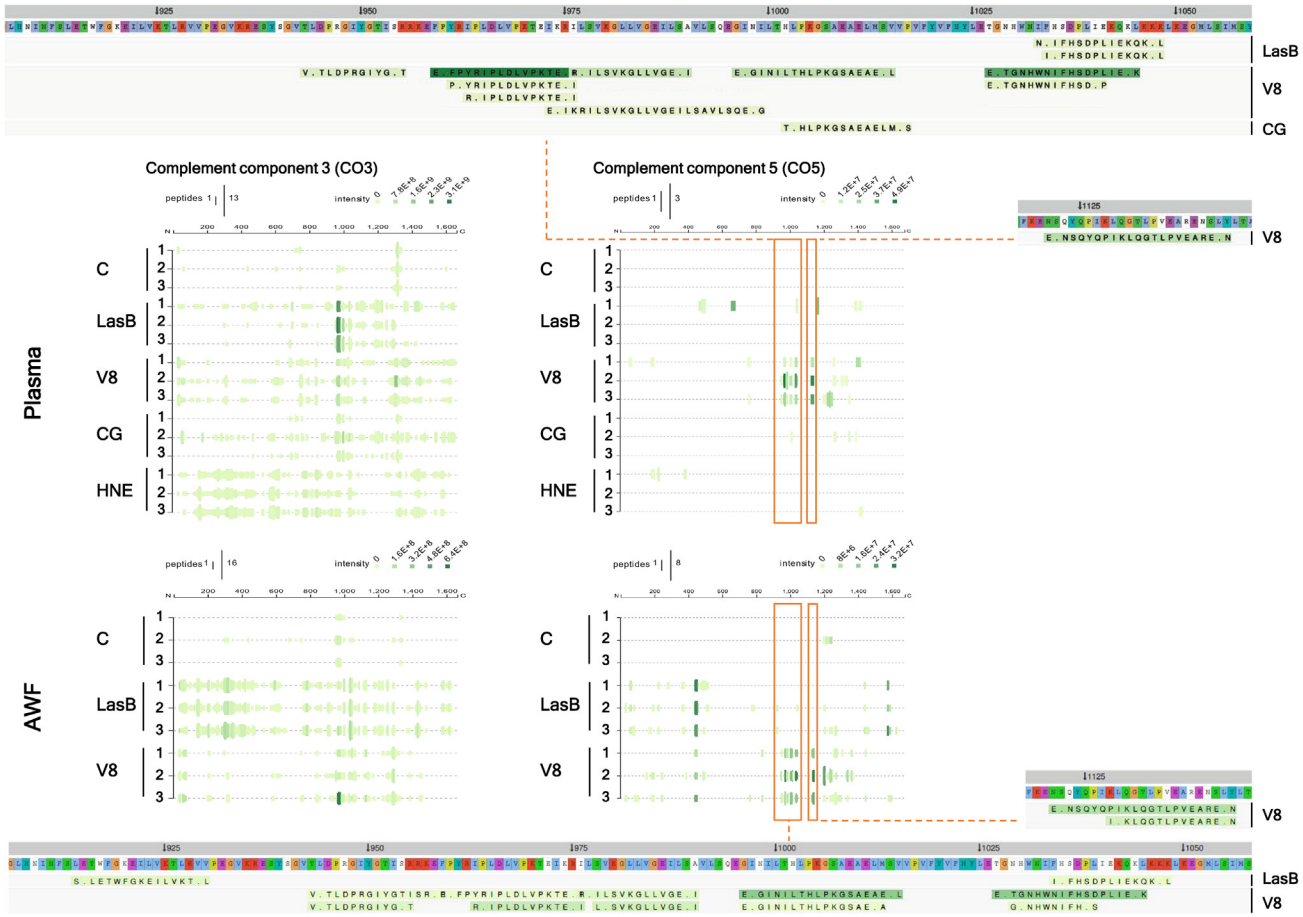


**Figure 7. Peptide profiles for complement factors**

Peptide profiles and peptide alignment maps were generated for the complement factors C3 and C5. Peptide regions unique to V8 treated samples are highlighted by orange boxes, and a selection of the corresponding peptides is shown for illustration purposes.

immunomodulatory properties,[50–52] whereas the heparin binding domain (residues 142–147) is responsible for cell attachment and cytotoxicity.[52,53] Here we show the formation of several ApoE peptides by both V8 and CG, although peptides spanning the antimicrobial and immunomodulatory region at residues 130–150 are not observed. Moreover, V8 cleaves between residues $^{139}$E-$^{140}$V, and CG between $^{132}$R-$^{133}$L, which may render peptides from this region inactive. In AWF, no peptides were found spanning this region either. Interestingly, the complete lack of peptides in the 'high' LasB and HNE samples, as can be observed in Figure 3A, suggests that these two enzymes can degrade ApoE beyond LC-MS/MS identification, which is also in agreement with the lack of ApoE peptides observed in inflamed, infected wounds.

Similar to ApoE, clusterin (CLUS/apolipoprotein J) is cleaved by V8 and CG, whereas no peptides were observed in any of the 'high' LasB and HNE samples, or in the samples of the infected wounds. Therefore, the lack of ApoE and clusterin may be a marker for a highly proteolytic environment as such.

## DISCUSSION

The clinical assessment of wound infection and related complications is challenging, as it is based on personal experience of the healthcare provider combined with bacterial detection. To complicate matters, the presence of bacteria does not necessarily result in infection and inflammation, whereas infection can be present in the absence of the classic infection signs, such as redness, heat, swelling, odor, purulent exudate and pain.[54–56] Therefore, the development of objective methods to measure wound status and predict healing outcomes is essential.[57] Currently, various approaches are under development, such as sensors to monitor pH and temperature.[58,59] Moreover, measurement of general elevated protease activity in clinics may be done using the Woundchek Protease status[12] and the Woundchek Bacterial status, developed by Woundchek Laboratories, although additional independent clinical studies are needed to further determine the diagnostic and prognostic value of these tests. As proteolytic activity is an indicator for the level of protein degradation, the identification of endogenous peptides may be useful to measure and predict wound healing status. Indeed, endogenous peptides may serve as biomarkers in a range of diseases.[60–63] To investigate the possibility of using peptides as biomarkers for wound status, we previously

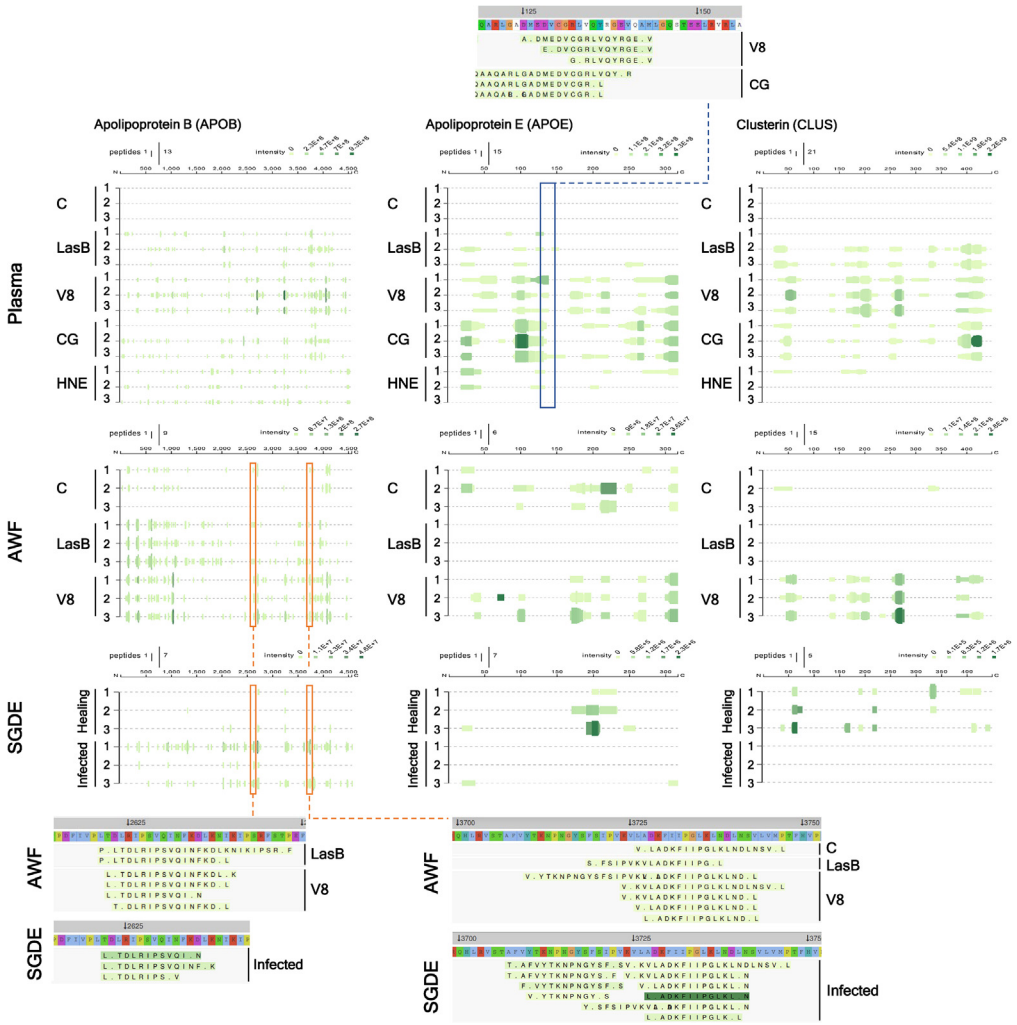


**Figure 8. Peptide profiles for apolipoproteins**

Peptide profiles and peptide alignment maps were generated for apolipoprotein B, apolipoprotein E, and clusterin. Interesting peptide regions are highlighted by orange and blue boxes, and a selection of the corresponding peptides is shown for illustration purposes. Top, plasma samples; middle, acute wound fluid (AWF) samples; bottom, skin graft dressing extracts (SGDE) from three healing, non-inflamed wounds and three *S. aureus* infected, high inflamed wounds from datasets obtained previously.[25]

developed a mass spectrometry-based method to measure the low-molecular-weight peptidome of wound fluids and used this method to identify unique peptides and patterns that differed between healing/non-infected and inflamed/infected wounds.[25,26] As individual proteases have different substrate specificities, and will result in peptides with enzyme specific sequences, the observed differences may be explained by the level and nature of individual proteases in these wounds, which may have additional diagnostic/prognostic value. Therefore, we set out to characterize the plasma and wound fluid targets of selected endogenous and bacterial proteases. We used digestion of plasma to mimic the endogenous formation of AWFs, whereas we used both plasma and AWFs from non-infected patients to investigate bacterial protease activity during wound infection. As a proof-of-concept, we chose four proteases that have been shown to play important roles in wound healing and infection, the two neutrophil-derived serine proteases HNE and CG, and two bacterial protease from respectively *S. aureus* and *P. aeruginosa*. Both HNE and CG are abundant endogenous proteases identified in healing and infected, non-healing wounds[10,26,64] and have been shown to be capable of degrading proteins of relevance for wound healing, including those of the extracellular matrix, such as elastin,[30] fibronectin,[65,66] and laminins.[18] Interestingly, our data reveals 127 plasma protein targets for HNE, and 102 for CG and show clear substrate specificity as only 39 of these protein targets where common for both enzymes. In agreement, analysis of the N- and C-terminal amino acids of the identified peptides revealed expected shifts in the peptide composition, as reported previously.[29–32] For LasB and V8, we found respectively 145 and 142 protein targets not detected in the control plasma samples, whereas these numbers were 155 for LasB and 180 for V8 in wound fluids. A recent report using N-terminomics revealed the detection of 85 host-protein targets of V8 in human serum,[17] many of which we identified here with our peptidomics approach as well, thereby showing the validity of our methods

and results. Nevertheless, we cannot exclude that some of the identified proteins are actually generated by other proteases present as proenzymes in the original samples, as proteases are known to release active proteases from their precursors.

Unique to peptidomics, investigation of the native peptide profiles revealed enzyme specific peptide patterns and identified unique peptide regions providing potential biomarker candidates. Of special interest are those found in fetuin-A (around amino acid residue 290) and ApoB (around amino acid residues 2700 and 3725), which were unique for V8 and identified in dressing extracts from *S. aureus* infected wounds. However, large scale studies of patient samples are needed to verify these results.

The lack of identification of specific proteins may be a marker of a high proteolytic environment as such, as observed for apolipoprotein E (ApoE) and clusterin. Further evidence for distinct proteolytic targets during infection is revealed in the heatmaps, as the bacterial proteases digested complement factors, immunoglobulins, protease inhibitors and ECM components. Moreover, the peptide profiles for ApoE, fibrinogen beta chain (FIBB), kininogen (KNG1), and the complement factors C3 and C5, reveal that both bacterial enzymes degraded the antibacterial regions of these proteins. Together, these actions will actively modulate the host environment and improve chances for successful infection. Interestingly, the endogenous proteases had similar targets, providing further evidence of the importance of balanced endogenous proteolytic activity in healing wounds to prevent infection.

From a technical perspective, it should be noted that our previously developed method was not optimal for the identification of peptides in plasma. Therefore, we changed the used extraction buffer from Urea with *Rapi*Gest to a GdCl buffer containing TCEP and CAA, which denatures, reduces, and alkylates cysteines and may induce some cleavage around cysteine residues.[67] As a consequence, we did not only identify significantly more peptides, but we also observed an increase in cysteine-containing peptides as reported previously,[68] which were almost absent in the wound fluid samples. Notably, the lack of identifying Cys containing peptides in peptidomics has been reported,[69] whereas the further amino acid composition of the identified peptides generally reflected the frequency in the Eukaryotic proteome. Therefore, care should be taken when comparing data generated with different buffers.

Importantly, as the presence of different concentrations of the same protease may lead to changes in the peptidomes, we selected two concentrations for each enzyme. Indeed, clear differences were observed when using the 'low' and 'high' amount of these proteases. For LasB and HNE, we found less peptides and proteins in the 'high' samples as compared to the 'low' samples, indicating extensive degradation, whereas for CG and V8 the opposite was observed. Moreover, there was a substantial difference in identified proteins and unique peptides between the two groups of each enzyme. This demonstrates the importance of selecting multiple enzyme concentrations in these types of studies.

Taken together, this study reveals a range of protease substrates in plasma and wound fluids, which may help elucidate biological roles during health and disease. Moreover, the peptidomics data reveals potential biomarker candidates for infected wounds, which should be verified in follow up studies with large scale patient cohorts. Finally, we provide a proof-of-concept that individual protease activity results in unique peptides and peptide patterns, that may be used for the discovery of novel peptide-based diagnostic and prognostic biomarker candidates in future studies on well-defined patient groups.

### Limitations of the study

A limitation of this study is the low sample size. In addition, in a physiological wound environment enzymatic activity is an ever-changing process, and many enzymes will contribute to the peptidome, making it challenging to translate findings with single enzymes and single time points. Nevertheless, the identification of peptide regions in the V8 samples that were also unique to dressing extracts of *S. aureus* infected wounds validates our approach. However, large scale studies of patient samples are needed to verify our results.

From a technical perspective, the lack of identification with our method could be due to either high levels or very low levels of degradation, as our method can only measure peptides between 500 and 8000 Dalton. Also, two cleavage sites on the same protein should be within close proximity, to obtain peptides within this range. In agreement, the apparent increase in average peptide length with 'high' levels of LasB, as compared to 'low' levels, is likely caused by fragmentation of larger proteins and peptides that were first above the detection level, in combination with the extensive degradation of smaller peptides, to below detection limit.

## STAR★METHODS

Detailed methods are provided in the online version of this paper and include the following:

- KEY RESOURCES TABLE
- RESOURCE AVAILABILITY
  - Lead contact
  - Materials availability
  - Data and code availability
- EXPERIMENTAL MODEL AND STUDY PARTICIPANT DETAILS
- METHOD DETAILS
  - *In vitro* digestion of plasma/acute wound fluids
  - SDS-gel electrophoresis
  - Peptide extraction
  - LC-MS/MS analysis
- QUANTIFICATION AND STATISTICAL ANALYSIS

## SUPPLEMENTAL INFORMATION

Supplemental information can be found online at https://doi.org/10.1016/j.isci.2024.109005.

## ACKNOWLEDGMENTS

We would like to thank Simonas Savickas and Erwin Schoof for expert technical assistance with the LC-MS/MS runs performed at the DTU Proteomics Core, Denmark. Furthermore, we thank Sven Kjellström at Lund University, Sweden, for access to and help with the PEAKS analysis software. The wound fluids were a kind gift of Artur Schmidtchen, Lund University, Sweden. This work was supported by grants from the LEO Foundation (LF15007 and LF18020). The funders had no role in study design, data collection and interpretation, or the decision to submit the work for publication.

## AUTHOR CONTRIBUTIONS

J.C. and M.v.d.P. designed the study. All authors were involved in the performance of experiments and/or the interpretation of the experimental results. J.C. and M.v.d.P. wrote the manuscript. All authors reviewed the manuscript.

## DECLARATION OF INTERESTS

The authors declare no competing interests.

Received: October 16, 2023
Revised: November 20, 2023
Accepted: January 19, 2024
Published: January 26, 2024

## REFERENCES

1. Johnson, T.R., Gómez, B.I., McIntyre, M.K., Dubick, M.A., Christy, R.J., Nicholson, S.E., and Burmeister, D.M. (2018). The Cutaneous Microbiome and Wounds: New Molecular Targets to Promote Wound Healing. Int. J. Mol. Sci. *19*, 2699. https://doi.org/10.3390/ijms19092699.
2. Gushiken, L.F.S., Beserra, F.P., Bastos, J.K., Jackson, C.J., and Pellizzon, C.H. (2021). Cutaneous wound healing: an update from physiopathology to current therapies. Life *11*, 665. https://doi.org/10.3390/life11070665.
3. Sen, C.K., Gordillo, G.M., Roy, S., Kirsner, R., Lambert, L., Hunt, T.K., Gottrup, F., Gurtner, G.C., and Longaker, M.T. (2009). Human skin wounds: a major and snowballing threat to public health and the economy. Wound Repair Regen. *17*, 763–771. https://doi.org/10.1111/j.1524-475X.2009.00543.x.
4. Sen, C.K. (2019). Human wounds and its burden: an updated compendium of estimates. Adv. Wound Care (New Rochelle) *8*, 39–48. https://doi.org/10.1089/wound.2019.0946.
5. International Consensus (2012). Optimising Wellbeing in People Living with a Wound. An Expert Working Group Review (Wounds International). http://www.woundsinternational.com.
6. McCarty, S.M., and Percival, S.L. (2013). Proteases and Delayed Wound Healing. Adv. Wound Care *2*, 438–447. https://doi.org/10.1089/wound.2012.0370.
7. Saleh, K., Strömdahl, A.C., Riesbeck, K., and Schmidtchen, A. (2019). Inflammation Biomarkers and Correlation to Wound Status After Full-Thickness Skin Grafting. Front. Med. *6*, 159. https://doi.org/10.3389/fmed.2019.00159.
8. Serena, T.E., Cullen, B.M., Bayliff, S.W., Gibson, M.C., Carter, M.J., Chen, L., Yaakov, R.A., Samies, J., Sabo, M., DeMarco, D., et al. (2016). Defining a new diagnostic assessment parameter for wound care: Elevated protease activity, an indicator of nonhealing, for targeted protease-modulating treatment. Wound Repair Regen. *24*, 589–595. https://doi.org/10.1111/wrr.12431.
9. Serena, T.E., Bayliff, S.W., Brosnan, P.J., DiMarco, D.T., Doner, B.A., Guthrie, D.A., Patel, K.D., Sabo, M.J., Samies, J.H., and Carter, M.J. (2021). Bacterial protease activity as a biomarker to assess the risk of non-healing in chronic wounds: Results from a multicentre randomised controlled clinical trial. Wound Repair Regen. *29*, 752–758. https://doi.org/10.1111/wrr.12941.
10. Hasmann, A., Gewessler, U., Hulla, E., Schneider, K.P., Binder, B., Francesko, A., Tzanov, T., Schintler, M., Van der Palen, J., Guebitz, G.M., and Wehrschuetz-Sigl, E. (2011). Sensor materials for the detection of human neutrophil elastase and cathepsin G activity in wound fluid. Exp. Dermatol. *20*, 508–513. https://doi.org/10.1111/j.1600-0625.2011.01256.x.
11. Yang, T., Pan, S.C., and Cheng, C.M. (2020). Paper-based human neutrophil elastase detection device for clinical wound monitoring. Lab Chip *20*, 2709–2716. https://doi.org/10.1039/d0lc00062k.
12. Lockmann, A., Schill, T., Hartmann, F., Grönemeyer, L.L., Holzkamp, R., Schön, M.P., and Thoms, K.M. (2018). Testing Elevated Protease Activity: Prospective Analysis of 160 Wounds. Adv. Skin Wound Care *31*, 82–88. https://doi.org/10.1097/01.Asw.0000527965.64870.03.
13. Gjødsbøl, K., Christensen, J.J., Karlsmark, T., Jørgensen, B., Klein, B.M., and Krogfelt, K.A. (2006). Multiple bacterial species reside in chronic wounds: a longitudinal study. Int. Wound J. *3*, 225–231. https://doi.org/10.1111/j.1742-481X.2006.00159.x.
14. Wolcott, R.D., Hanson, J.D., Rees, E.J., Koenig, L.D., Phillips, C.D., Wolcott, R.A., Cox, S.B., and White, J.S. (2016). Analysis of the chronic wound microbiota of 2,963 patients by 16S rDNA pyrosequencing. Wound Repair Regen. *24*, 163–174. https://doi.org/10.1111/wrr.12370.
15. Dowd, S.E., Sun, Y., Secor, P.R., Rhoads, D.D., Wolcott, B.M., James, G.A., and Wolcott, R.D. (2008). Survey of bacterial diversity in chronic wounds using pyrosequencing, DGGE, and full ribosome shotgun sequencing. BMC Microbiol. *8*, 43. https://doi.org/10.1186/1471-2180-8-43.
16. Beaufort, N., Corvazier, E., Hervieu, A., Choqueux, C., Dussiot, M., Louedec, L., Cady, A., de Bentzmann, S., Michel, J.B., and Pidard, D. (2011). The thermolysin-like metalloproteinase and virulence factor LasB from pathogenic Pseudomonas aeruginosa induces anoikis of human vascular cells. Cell Microbiol. *13*, 1149–1167. https://doi.org/10.1111/j.1462-5822.2011.01606.x.
17. Frey, A.M., Chaput, D., and Shaw, L.N. (2021). Insight into the human pathodegradome of the V8 protease from Staphylococcus aureus. Cell Rep. *35*, 108930. https://doi.org/10.1016/j.celrep.2021.108930.
18. Senyürek, I., Kempf, W.E., Klein, G., Maurer, A., Kalbacher, H., Schäfer, L., Wanke, I., Christ, C., Stevanovic, S., Schaller, M., et al. (2014). Processing of laminin α chains generates peptides involved in wound healing and host defense. J. Innate Immun. *6*, 467–484. https://doi.org/10.1159/000357032.
19. Morihara, K., Tsuzuki, H., and Oda, K. (1979). Protease and elastase of Pseudomonas aeruginosa: inactivation of human plasma alpha 1-proteinase inhibitor. Infect. Immun. *24*, 188–193. https://doi.org/10.1128/iai.24.1.188-193.1979.
20. Schmidtchen, A., Holst, E., Tapper, H., and Björck, L. (2003). Elastase-producing Pseudomonas aeruginosa degrade plasma proteins and extracellular products of human skin and fibroblasts, and inhibit fibroblast growth. Microb. Pathog. *34*, 47–55. https://doi.org/10.1016/s0882-4010(02)00197-3.

21. van der Plas, M.J.A., Bhongir, R.K.V., Kjellström, S., Siller, H., Kasetty, G., Mörgelin, M., and Schmidtchen, A. (2016). Pseudomonas aeruginosa elastase cleaves a C-terminal peptide from human thrombin that inhibits host inflammatory responses. Nat. Commun. *7*, 11567. https://doi.org/10.1038/ncomms11567.
22. Okamoto, T., Akaike, T., Suga, M., Tanase, S., Horie, H., Miyajima, S., Ando, M., Ichinose, Y., and Maeda, H. (1997). Activation of human matrix metalloproteinases by various bacterial proteinases. J. Biol. Chem. *272*, 6059–6066. https://doi.org/10.1074/jbc.272.9.6059.
23. Pietrocola, G., Nobile, G., Rindi, S., and Speziale, P. (2017). Staphylococcus aureus Manipulates Innate Immunity through Own and Host-Expressed Proteases. Front. Cell. Infect. Microbiol. *7*, 166. https://doi.org/10.3389/fcimb.2017.00166.
24. Sorsa, T., Ingman, T., Suomalainen, K., Haapasalo, M., Konttinen, Y.T., Lindy, O., Saari, H., and Uitto, V.J. (1992). Identification of proteases from periodontopathogenic bacteria as activators of latent human neutrophil and fibroblast-type interstitial collagenases. Infect. Immun. *60*, 4491–4495. https://doi.org/10.1128/iai.60.11.4491-4495.1992.
25. van der Plas, M.J., Cai, J., Petrlova, J., Saleh, K., Kjellström, S., and Schmidtchen, A. (2021). Method development and characterisation of the low-molecular-weight peptidome of human wound fluids. Elife *10*, e66876. https://doi.org/10.7554/eLife.66876.
26. Hartman, E., Wallblom, K., van der Plas, M.J.A., Petrlova, J., Cai, J., Saleh, K., Kjellström, S., and Schmidtchen, A. (2020). Bioinformatic Analysis of the Wound Peptidome Reveals Potential Biomarkers and Antimicrobial Peptides. Front. Immunol. *11*, 620707. https://doi.org/10.3389/fimmu.2020.620707.
27. Colaert, N., Helsens, K., Martens, L., Vandekerckhove, J., and Gevaert, K. (2009). Improved visualization of protein consensus sequences by iceLogo. Nat. Methods *6*, 786–787. https://doi.org/10.1038/nmeth1109-786.
28. Drapeau, G.R., Boily, Y., and Houmard, J. (1972). Purification and Properties of an Extracellular Protease of Staphylococcus aureus. J. Biol. Chem. *247*, 6720–6726. https://doi.org/10.1016/S0021-9258(19)44749-2.
29. Thorpe, M., Fu, Z., Chahal, G., Akula, S., Kervinen, J., de Garavilla, L., and Hellman, L. (2018). Extended cleavage specificity of human neutrophil cathepsin G: A low activity protease with dual chymase and tryptase-type specificities. PLoS One *13*, e0195077. https://doi.org/10.1371/journal.pone.0195077.
30. Heinz, A., Jung, M.C., Jahreis, G., Rusciani, A., Duca, L., Debelle, L., Weiss, A.S., Neubert, R.H.H., and Schmelzer, C.E.H. (2012). The action of neutrophil serine proteases on elastin and its precursor. Biochimie *94*, 192–202. https://doi.org/10.1016/j.biochi.2011.10.006.
31. Fu, Z., Thorpe, M., Akula, S., Chahal, G., and Hellman, L.T. (2018). Extended Cleavage Specificity of Human Neutrophil Elastase, Human Proteinase 3, and Their Distant Ortholog Clawed Frog PR3-Three Elastases With Similar Primary but Different Extended Specificities and Stability. Front. Immunol. *9*, 2387. https://doi.org/10.3389/fimmu.2018.02387.
32. Schilling, O., and Overall, C.M. (2008). Proteome-derived, database-searchable peptide libraries for identifying protease cleavage sites. Nat. Biotechnol. *26*, 685–694. https://doi.org/10.1038/nbt1408.
33. Rawlings, N.D., Waller, M., Barrett, A.J., and Bateman, A. (2014). MEROPS: the database of proteolytic enzymes, their substrates and inhibitors. Nucleic Acids Res. *42*, D503–D509. https://doi.org/10.1093/nar/gkt953.
34. Kearney, K.J., Ariëns, R.A.S., and Macrae, F.L. (2022). The Role of Fibrin(ogen) in Wound Healing and Infection Control. Semin. Thromb. Hemost. *48*, 174–187. https://doi.org/10.1055/s-0041-1732467.
35. Påhlman, L.I., Mörgelin, M., Kasetty, G., Olin, A.I., Schmidtchen, A., and Herwald, H. (2013). Antimicrobial activity of fibrinogen and fibrinogen-derived peptides–a novel link between coagulation and innate immunity. Thromb. Haemostasis *109*, 930–939. https://doi.org/10.1160/th12-10-0739.
36. Schmaier, A.H., Zuckerberg, A., Silverman, C., Kuchibhotla, J., Tuszynski, G.P., and Colman, R.W. (1983). High-molecular weight kininogen. A secreted platelet protein. J. Clin. Invest. *71*, 1477–1489. https://doi.org/10.1172/jci110901.
37. Kozik, A., Moore, R.B., Potempa, J., Imamura, T., Rapala-Kozik, M., and Travis, J. (1998). A novel mechanism for bradykinin production at inflammatory sites. Diverse effects of a mixture of neutrophil elastase and mast cell tryptase versus tissue and plasma kallikreins on native and oxidized kininogens. J. Biol. Chem. *273*, 33224–33229. https://doi.org/10.1074/jbc.273.50.33224.
38. Nordahl, E.A., Rydengård, V., Mörgelin, M., and Schmidtchen, A. (2005). Domain 5 of high molecular weight kininogen is antibacterial. J. Biol. Chem. *280*, 34832–34839. https://doi.org/10.1074/jbc.M507249200.
39. Wang, H., and Sama, A.E. (2012). Anti-inflammatory role of fetuin-A in injury and infection. Curr. Mol. Med. *12*, 625–633. https://doi.org/10.2174/156652412800620039.
40. Wozniak, J.M., Mills, R.H., Olson, J., Caldera, J.R., Sepich-Poore, G.D., Carrillo-Terrazas, M., Tsai, C.M., Vargas, F., Knight, R., Dorrestein, P.C., et al. (2020). Mortality Risk Profiling of Staphylococcus aureus Bacteremia by Multi-omic Serum Analysis Reveals Early Predictive and Pathogenic Signatures. Cell *182*, 1311–1327.e14. https://doi.org/10.1016/j.cell.2020.07.040.
41. Li, W., Zhu, S., Li, J., Huang, Y., Zhou, R., Fan, X., Yang, H., Gong, X., Eissa, N.T., Jahnen-Dechent, W., et al. (2011). A hepatic protein, fetuin-A, occupies a protective role in lethal systemic inflammation. PLoS One *6*, e16945. https://doi.org/10.1371/journal.pone.0016945.
42. Defendi, F., Thielens, N.M., Clavarino, G., Cesbron, J.Y., and Dumestre-Pérard, C. (2020). The Immunopathology of Complement Proteins and Innate Immunity in Autoimmune Disease. Clin. Rev. Allergy Immunol. *58*, 229–251. https://doi.org/10.1007/s12016-019-08774-5.
43. Jusko, M., Potempa, J., Kantyka, T., Bielecka, E., Miller, H.K., Kalinska, M., Dubin, G., Garred, P., Shaw, L.N., and Blom, A.M. (2014). Staphylococcal proteases aid in evasion of the human complement system. J. Innate Immun. *6*, 31–46. https://doi.org/10.1159/000351458.
44. Schultz, D.R., and Miller, K.D. (1974). Elastase of Pseudomonas aeruginosa: inactivation of complement components and complement-derived chemotactic and phagocytic factors. Infect. Immun. *10*, 128–135. https://doi.org/10.1128/iai.10.1.128-135.1974.
45. Dominiczak, M.H., and Caslake, M.J. (2011). Apolipoproteins: metabolic role and clinical biochemistry applications. Ann. Clin. Biochem. *48*, 498–515. https://doi.org/10.1258/acb.2011.011111.
46. Peterson, M.M., Mack, J.L., Hall, P.R., Alsup, A.A., Alexander, S.M., Sully, E.K., Sawires, Y.S., Cheung, A.L., Otto, M., and Gresham, H.D. (2008). Apolipoprotein B Is an innate barrier against invasive Staphylococcus aureus infection. Cell Host Microbe *4*, 555–566. https://doi.org/10.1016/j.chom.2008.10.001.
47. Petruk, G., Elvén, M., Hartman, E., Davoudi, M., Schmidtchen, A., Puthia, M., and Petrlova, J. (2021). The role of full-length apoE in clearance of Gram-negative bacteria and their endotoxins. J. Lipid Res. *62*, 100086. https://doi.org/10.1016/j.jlr.2021.100086.
48. Dobson, C.B., Sales, S.D., Hoggard, P., Wozniak, M.A., and Crutcher, K.A. (2006). The receptor-binding region of human apolipoprotein E has direct anti-infective activity. J. Infect. Dis. *193*, 442–450. https://doi.org/10.1086/499280.
49. Forbes, S., McBain, A.J., Felton-Smith, S., Jowitt, T.A., Birchenough, H.L., and Dobson, C.B. (2013). Comparative surface antimicrobial properties of synthetic biocides and novel human apolipoprotein E derived antimicrobial peptides. Biomaterials *34*, 5453–5464. https://doi.org/10.1016/j.biomaterials.2013.03.087.
50. Pane, K., Sgambati, V., Zanfardino, A., Smaldone, G., Cafaro, V., Angrisano, T., Pedone, E., Di Gaetano, S., Capasso, D., Haney, E.F., et al. (2016). A new cryptic cationic antimicrobial peptide from human apolipoprotein E with antibacterial activity and immunomodulatory effects on human cells. FEBS J *283*, 2115–2131. https://doi.org/10.1111/febs.13725.
51. Wang, C.Q., Yang, C.S., Yang, Y., Pan, F., He, L.Y., and Wang, A.M. (2013). An apolipoprotein E mimetic peptide with activities against multidrug-resistant bacteria and immunomodulatory effects. J. Pept. Sci. *19*, 745–750. https://doi.org/10.1002/psc.2570.
52. Clay, M.A., Anantharamaiah, G.M., Mistry, M.J., Balasubramaniam, A., and Harmony, J.A. (1995). Localization of a domain in apolipoprotein E with both cytostatic and cytotoxic activity. Biochemistry *34*, 11142–11151. https://doi.org/10.1021/bi00035a020.
53. Saito, H., Dhanasekaran, P., Nguyen, D., Baldwin, F., Weisgraber, K.H., Wehrli, S., Phillips, M.C., and Lund-Katz, S. (2003). Characterization of the heparin binding sites in human apolipoprotein. J. Biol. Chem. *278*, 14782–14787. https://doi.org/10.1074/jbc.M213207200.
54. Saleh, K., and Schmidtchen, A. (2015). Surgical site infections in dermatologic surgery: etiology, pathogenesis, and current preventative measures. Dermatol. Surg. *41*, 537–549. https://doi.org/10.1097/dss.0000000000000364.
55. (2008). Wound infection in clinical practice. An international consensus. Int. Wound J. *5* (*Suppl 3*). iii–11. https://doi.org/10.1111/j.1742-481X.2008.00488.x.

56. Siddiqui, A.R., and Bernstein, J.M. (2010). Chronic wound infection: facts and controversies. Clin. Dermatol. *28*, 519–526. https://doi.org/10.1016/j.clindermatol.2010.03.009.
57. WUWHS (2008). World Union of Wound Healing Societies (WUWHS). Principles of Best Practice: Diagnostics and Wounds. A Consensus Document (MEP Ltd).
58. Tang, N., Zheng, Y., Jiang, X., Zhou, C., Jin, H., Jin, K., Wu, W., and Haick, H. (2021). Wearable Sensors and Systems for Wound Healing-Related pH and Temperature Detection. Micromachines *12*, 430. https://doi.org/10.3390/mi12040430.
59. Sun, X., Zhang, Y., Ma, C., Yuan, Q., Wang, X., Wan, H., and Wang, P. (2021). A Review of Recent Advances in Flexible Wearable Sensors for Wound Detection Based on Optical and Electrical Sensing. Biosensors *12*, 10. https://doi.org/10.3390/bios12010010.
60. Falconi-Agapito, F., Kerkhof, K., Merino, X., Bakokimi, D., Torres, F., Van Esbroeck, M., Talledo, M., and Ariën, K.K. (2022). Peptide Biomarkers for the Diagnosis of Dengue Infection. Front. Immunol. *13*, 793882. https://doi.org/10.3389/fimmu.2022.793882.
61. Abid, M.S.R., Qiu, H., Tripp, B.A., de Lima Leite, A., Roth, H.E., Adamec, J., Powers, R., and Checco, J.W. (2022). Peptidomics analysis reveals changes in small urinary peptides in patients with interstitial cystitis/bladder pain syndrome. Sci. Rep. *12*, 8289. https://doi.org/10.1038/s41598-022-12197-2.
62. Zhao, Y., Tong, D., Wang, M., Xu, C., Gong, X., Wang, Z., and Li, C. (2022). Peptidomics Analysis Reveals Serum Biomarkers in Spinal Cord Injury Patients. Crit. Rev. Eukaryot. Gene Expr. *32*, 1–9. https://doi.org/10.1615/CritRevEukaryotGeneExpr.2021039575.
63. Greening, D.W., Kapp, E.A., and Simpson, R.J. (2017). The Peptidome Comes of Age: Mass Spectrometry-Based Characterization of the Circulating Cancer Peptidome. Enzymes *42*, 27–64. https://doi.org/10.1016/bs.enz.2017.08.003.
64. Herrick, S., Ashcroft, G., Ireland, G., Horan, M., McCollum, C., and Ferguson, M. (1997). Up-regulation of elastase in acute wounds of healthy aged humans and chronic venous leg ulcers are associated with matrix degradation. Lab. Invest. *77*, 281–288.
65. Son, E.D., Kim, H., Choi, H., Lee, S.H., Lee, J.Y., Kim, S., Closs, B., Lee, S., Chung, J.H., and Hwang, J.S. (2009). Cathepsin G increases MMP expression in normal human fibroblasts through fibronectin fragmentation, and induces the conversion of proMMP-1 to active MMP-1. J. Dermatol. Sci. *53*, 150–152. https://doi.org/10.1016/j.jdermsci.2008.08.006.
66. Grinnell, F., and Zhu, M. (1994). Identification of neutrophil elastase as the proteinase in burn wound fluid responsible for degradation of fibronectin. J. Invest. Dermatol. *103*, 155–161. https://doi.org/10.1111/1523-1747.ep12392625.
67. Liu, P., O'Mara, B.W., Warrack, B.M., Wu, W., Huang, Y., Zhang, Y., Zhao, R., Lin, M., Ackerman, M.S., Hocknell, P.K., et al. (2010). A Tris (2-Carboxyethyl) Phosphine (TCEP) Related Cleavage on Cysteine-Containing Proteins. J. Am. Soc. Mass Spectrom. *21*, 837–844. https://doi.org/10.1016/j.jasms.2010.01.016.
68. Sechi, S., and Chait, B.T. (1998). Modification of cysteine residues by alkylation. A tool in peptide mapping and protein identification. Anal. Chem. *70*, 5150–5158. https://doi.org/10.1021/ac9806005.
69. Fricker, L.D. (2015). Limitations of Mass Spectrometry-Based Peptidomic Approaches. J. Am. Soc. Mass Spectrom. *26*, 1981–1991. https://doi.org/10.1007/s13361-015-1231-x.
70. Lundqvist, K., Herwald, H., Sonesson, A., and Schmidtchen, A. (2004). Heparin binding protein is increased in chronic leg ulcer fluid and released from granulocytes by secreted products of Pseudomonas aeruginosa. Thromb. Haemostasis *92*, 281–287. https://doi.org/10.1160/th03-12-0732.
71. UniProt Consortium (2023). UniProt: the Universal Protein Knowledgebase in 2023. Nucleic Acids Res. *51*, D523–D531. https://doi.org/10.1093/nar/gkac1052.
72. Ignatchenko, V., Ignatchenko, A., Sinha, A., Boutros, P.C., and Kislinger, T. (2015). VennDIS: a JavaFX-based Venn and Euler diagram software to generate publication quality figures. Proteomics *15*, 1239–1244. https://doi.org/10.1002/pmic.201400320.
73. Spitzer, M., Wildenhain, J., Rappsilber, J., and Tyers, M. (2014). BoxPlotR: a web tool for generation of box plots. Nat. Methods *11*, 121–122. https://doi.org/10.1038/nmeth.2811.
74. Manguy, J., Jehl, P., Dillon, E.T., Davey, N.E., Shields, D.C., and Holton, T.A. (2017). Peptigram: A Web-Based Application for Peptidomics Data Visualization. J. Proteome Res. *16*, 712–719. https://doi.org/10.1021/acs.jproteome.6b00751.
75. Kalogeropoulos, K., Haack, A.M., Madzharova, E., Di Lorenzo, A., Hanna, R., Schoof, E.M., and auf dem Keller, U. (2023). CLIPPER 2.0: Peptide level annotation and data analysis for positional proteomics. Preprint at bioRxiv. https://doi.org/10.1101/2023.11.30.569335.
76. Perez-Riverol, Y., Csordas, A., Bai, J., Bernal-Llinares, M., Hewapathirana, S., Kundu, D.J., Inuganti, A., Griss, J., Mayer, G., Eisenacher, M., et al. (2019). The PRIDE database and related tools and resources in 2019: improving support for quantification data. Nucleic Acids Res. *47*, D442–D450. https://doi.org/10.1093/nar/gky1106.

## STAR★METHODS

### KEY RESOURCES TABLE

| REAGENT or RESOURCE | SOURCE | IDENTIFIER |
|---|---|---|
| Biological samples | | |
| Plasma from citrated blood | Healthy volunteers | N/A |
| Sterile acute wound fluids | Prof Artur Schmidtchen, Lund University, Sweden[25,26,70] | N/A |
| Chemicals, peptides, and recombinant proteins | | |
| Pseudomonas aeruginosa elastase | Elastin Products Company, Inc. | Cat#PE961 |
| Staphylococcus aureus V8 | Sigma-Aldrich | Cat#P2922 |
| Human neutrophil elastase | Sigma-Aldrich | Cat#324681 |
| Human neutrophil cathepsin G | Sigma-Aldrich | Cat#219373 |
| NuPAGE LDS sample buffer (4x) | Invitrogen™ | Cat#NP0007 |
| Tris-Glycine SDS running buffer (10x) | Invitrogen™ | Cat#LC2675 |
| *Rapi*Gest SF | Waters | Cat#186001861 |
| Critical commercial assays | | |
| Pierce™ BCA Protein Assay Kit | Thermo Scientific™ | Cat#23227 |
| Novex™ Tris-Glycine Mini Protein Gels, 10-20% | Invitrogen™ | Cat#XP10205BOX |
| SilverQuest™ Silver Staining Kit | Invitrogen™ | Cat#LC6070 |
| Deposited data | | |
| Mass spectrometry RAW data plasma samples | This paper | PRIDE: PXD037245 |
| Mass spectrometry RAW data wound fluids | This paper | PRIDE: PXD037047 |
| PEAKS search files plasma samples | This paper | PRIDE: PXD037245 |
| PEAKS search files wound fluids | This paper | PRIDE: PXD037047 |
| Mass spectrometry data of wound dressing extracts | Hartman et al.[26] | PRIDE: PXD023244 |
| UniProt | The UniProt Consortium[71] | https://www.uniprot.org/ |
| Software and algorithms | | |
| PEAKS Software | Bioinformatics Solutions Inc. | https://www.bioinfor.com/peaks-software/ |
| Graphpad Prism | Dotmatics | https://www.graphpad.com/ |
| VennDis | Ignatchenko et al.[72] | http://kislingerlab.uhnres.utoronto.ca/projects/ |
| BoxPlotR | Spitzer et al.[73] | http://shiny.chemgrid.org/boxplotr/ |
| Imgflip | Imgflip LLC | https://imgflip.com/chart-maker |
| Peptigram | Manguy et al.[74] | http://bioware.ucd.ie/peptigram/ |
| iceLogo | Colaert et al.[27] | http://iomics.ugent.be/icelogoserver/ |
| CLIPPER 2.0 | Kalogeropoulos et al.[75] | https://github.com/UadKLab/CLIPPER-2.0 |
| Other | | |
| Microcon-30kDa centrifugal filters | Merck | Cat#MRCF0R030 |

## RESOURCE AVAILABILITY

### Lead contact

Further information and requests for resources should be directed to and will be fulfilled by the lead contact, Mariena van der Plas (mariena.van_der_plas@sund.ku.dk).

### Materials availability

This study did not generate new unique reagents.

### Data and code availability

- The mass spectrometry data have been deposited to the ProteomeXchange consortium via the PRIDE[76] partner repository with the dataset identifiers PXD037245 (plasma) and PXD037047 (acute wound fluid). This paper also analyses existing, publicly available data with dataset identifier PXD023244.
- This paper does not report original code.
- Any additional information required to reanalyse the data reported in this paper is available from the lead contact upon request.

## EXPERIMENTAL MODEL AND STUDY PARTICIPANT DETAILS

Plasma was collected from citrated venous blood from three healthy female donors after 10 min centrifugation at 2000 g. The protocol for the collection of human plasma from blood (permit DNR2015/801) was approved by the Ethics Committee at Lund University. The human sterile acute wound fluids, obtained from surgical drainages after mastectomy,[70] were a kind gift from Professor Artur Schmidtchen (Lund University). Informed consent was obtained from all subjects. All samples were aliquoted and stored at −20°C before use.

Notably, although all samples were derived from adult females with European ancestry, this does not bias the results, as sex or age does not change protein sequences as such. Nevertheless, ethnicity related polymorphisms in individual protein sequences at cleavage sites cannot be excluded.

## METHOD DETAILS

### *In vitro* digestion of plasma/acute wound fluids

Due to large variations in protein content of the donor fluids (plasma samples ranged from 34.9 to 61.6 mg/ml; acute wound fluid samples ranged from 33.3 to 41.3 mg/ml), as measured by using the Pierce BCA Protein Assay Kit (Thermo Scientific, USA) according to manufacturer's instructions, sample protein content was normalized. For this purpose, 2.7 mg of plasma or acute wound fluid were mixed with 10 mM Tris buffer (pH 7.4), with or without the proteases *P. aeruginosa* elastase B (Elastin Products Company, Inc., USA), *S. aureus* V8 protease (Sigma-Aldrich, Germany), human neutrophil elastase (Sigma-Aldrich) or human neutrophil cathepsin G (Sigma-Aldrich), to obtain a total volume of 250 µl. Next, the samples were incubated for 24 h at 37°C, followed by SDS-PAGE analysis directly or storage at -80°C before peptide extraction and LC-MS/MS analysis.

### SDS-gel electrophoresis

*In vitro* digested and undigested samples (6 µg) were denatured at 95°C for 5 min in NuPAGE LDS Sample Buffer followed by separation on 10-20% Tris-Glycine mini gels in 1 x Tris-Glycine SDS running buffer at 225 V for 40 min. Gels and buffers were from Invitrogen (USA). Afterwards, gels were stained with the SilverQuest Staining kit (ThermoFisher, USA) according to manufacturer's instructions and visualized on a Gel Doc™ Imager (Bio-Rad Laboratories, USA).

### Peptide extraction

Acute wound fluid and plasma samples (250 µL) were defrosted and mixed with 750 µl freshly made urea (6 M final concentration in 10 mM Tris, pH 7.4) supplemented with *Rapi*Gest SF (0.05% final concentration; Waters, USA) followed by incubation for 30 min at room temperature,[25] or with 750 µl GdCl buffer containing 6 M guanidinium chloride (GdCl), 10 mM tris (2-carboxyethyl) phosphine (TCEP) and 40 mM 2-chloroacetamide (CAA) in 50 mM HEPES buffer at pH 8.5. Next, centrifugal filters with 30 kDa cut-off (Microcon 30, regenerated cellulose, Millipore, Ireland) were loaded with sample and centrifuged at 10000 g for 20 min at RT, then washed with 200 µl buffer followed by another 20 min centrifugation (10000 g at RT). Finally, the filtrates of both centrifugation steps were pooled and stored at -80°C before analysis by liquid chromatography tandem mass spectrometry (LC-MS/MS).

### LC-MS/MS analysis

Before LC-MS/MS analysis, 80 µl of each peptide extract was acidified with 40 µl 2% TFA and then trapped and enriched on StageTip columns. In short, columns were activated first by MeOH, then 80% ACN and 0.1% FA, and finally with 3% ACN and 1% TFA. Next, peptides were trapped on the column, washed with 0.1% FA, eluted with 40% ACN and 0.1% FA, and dried down before reconstitution in 2% ACN and 1% TFA with iRT peptides. Sample concentrations were measured using a nanodrop spectrophotometer (DeNovix, USA), and 500 ng was injected for LC-MS/MS analysis. For each sample, peptides were loaded onto a 2 cm C18 trap column (ThermoFisher 164705), connected in-line to a 50 cm C18 reverse-phase analytical column (Thermo EasySpray ES803) using 100% Buffer A (0.1% FA) at 750 bar, using the Thermo Easy-nLC 1200 HPLC system, and the column oven operating at 45°C. Peptides were first eluted over a 140 minute gradient ranging from 6% to 60% of 80% ACN, 0.1% FA at 250 nl/min, then they were introduced to the Orbitrap Eclipse Tribrid instrument (Thermo Fisher Scientific) coupled to FAIMSPro interface (Thermo Scientific, FMS02-10001) with a compensation voltage (CV) of either -50 or -70V, and were run in a DD-MS2 top speed method. Full MS spectra were collected at a resolution of 120,000, with an AGC target of $4\times10^5$ or maximum injection time of

50 ms and a scan range of 400–1500 m/z. The MS2 spectra were obtained in the ion trap operating at rapid speed, with an AGC target value of $1 \times 10^4$ or maximum injection time of 35 ms, a normalised HCD collision energy of 30 and an intensity threshold of $1.7e^4$. Dynamic exclusion was set to 60 s, and ions with a charge state <2, >7 or unknown were excluded. MS performance was verified for consistency by running quality control standards, and chromatography was monitored to check for reproducibility.

## QUANTIFICATION AND STATISTICAL ANALYSIS

MS/MS spectra were searched by PEAKS software. UniProt Human including 20,384 entries was used with nonspecific cleavage, 5 ppm precursor tolerance and 0.5 Da fragment tolerance for all samples. Oxidation (M) and deamidation (NQ) were treated as dynamic modification for AWFs and plasma samples, while carbamidomethyl (C) was used as a static modification for all plasma samples due to the use of GdCl buffer containing CAA. Search results were filtered based on PEAKS peptide score (a 25 score for the AWF samples and a 26 score for the CP samples), and at least two unique peptides for each protein.

For data visualization, heatmaps were generated by GraphPad Prism version 9 , venn diagrams were made in VennDis,[72] boxplots were made in BoxPlotR,[73] pie charts were made in Imgflip (https://imgflip.com/chart-maker), while peptide profiles and peptide alignment maps were made using the web-based application Peptigram.[74] Finally, iceLogos were generated using the iceLogo server,[27] using the cleavage environment of the detected peptides obtained with CLIPPER 2.0.[75] For this purpose, the Uniprot database[71] was used to retrieve the full protein sequences of the identified peptides. These sequences were used to extract the four preceding or the four following residues around the N-terminal and C-terminal cleavage sites for each peptide. These cleavage environments, spanning 8 residues across the cleavage site, were pooled for each condition, and the resulting cleavage list was used as input in Icelogo. Cleavage specificity logos were visualized as percentage change compared to background residue distribution, with the non-digested 24 h control samples or the Homo sapiens Swiss-Prot compiled residue frequency as background proteome.